The dynamic structure of liquid sodium from ab initio simulation

1994 J. Phys.: Condens. Matter 6 5231

(http://iopscience.iop.org/0953-8984/6/28/002)

J. Phys.: Condens. Matter 6 (1994) 5231–5241. Printed in the UK

The dynamic structure of liquid sodium from *ab initio* simulation

M Foley, E Smargiassi and P A Madden

Physical Chemistry Laboratory, Oxford University, South Parks Road, Oxford OX1 3QZ, UK

Received 7 April 1994

Abstract. Data that pertain to experimental x-ray and inelastic neutron scattering studies of liquid sodium are obtained from an *ab initio* molecular dynamics simulation. A long run was used, so the statistical precision of the calculated quantities is as good as obtained experimentally. The long run is made possible by the use of a recently developed modification of the Car–Parrinello method which uses an orbital-free density functional to prescribe the electron energetics. Agreement with experiment is excellent.

1. Introduction

Ab initio molecular dynamics simulations, as pioneered by Car and Parrinello [1], have greatly expanded the range of physical systems which can be accurately represented in computer simulations [2]. In this method the nuclear and electronic degrees of freedom describing the system are treated on the same footing. In most practical calculations the electronic degrees of freedom are the coefficients in the expansion of occupied orbitals in some basis set within the Kohn–Sham realization of density functional theory [3] and evolve simultaneously in time with the nuclear motion [4]. However, because of the amount of computer time required for the computations, calculations of properties on systems of 100 atoms or more and which require long runs, either for statistical averaging (such as free energies) or to study relatively slow dynamical processes, have not been made.

The computational cost arises from two sources. Firstly, the appropriate timestep in the CP integration is dictated by the fast dynamics of the orbital coefficients [5]. Secondly, because of the requirement that the occupied orbitals be kept orthogonal, the cost of a single timestep scales as N^2M for large systems, where M is the basis size and N the number of electrons. These problems are not circumvented by performing calculations with a timestep dictated by the nuclear motion and re-optimizing the wavefunction at each step [6]. The cost of a single iteration has the same poor scaling behaviour and the number of iterations required to achieve convergence depends on the nature and size of the system.

Various ways of overcoming the scaling problem have been suggested (so-called 'order N' methods). Most [7, 8, 9] depend on schemes which are appropriate when the electronic density matrix is short ranged, which is true for systems in which there is an energy gap between the occupied and virtual Kohn–Sham orbitals. We have followed a different approach [10], which, for the purpose of modelling the electronic behaviour of the system, uses an orbital-free density functional rather than the usual Kohn–Sham methodology. Such an approach is explicitly of order N for each electronic step. We have found suitable functionals for metals [11], for which the density matrix decays algebraically,

0953-8984/94/285231+11$19.50

so that the method is, at present, complementary to the other order N methods which have been introduced. A further advantage over the Kohn–Sham scheme for metals is that the electronic degrees of freedom behave adiabatically [10], a point which we further illustrate below. With the density as the basic variable we have shown that the electronic timestep is significantly longer than with a Kohn–Sham scheme and can be made *independent of system size*, so that the method is a *true* order N method for dynamics.

This opens the prospect of obtaining types of data which have hitherto been unavailable from *ab initio* molecular dynamics simulations. In this paper, we demonstrate that *ab initio* methods can be used to generate dynamical information at the level of experimental accuracy and precision. Elsewhere, we illustrate the application to free energy calculations [12].

2. Simulation method

The method used, which is exactly as described in [10], will be outlined here. We represent the system being studied as a set of ions in a cloud of valence electrons, with the spatial density distribution of this cloud, $\rho(r)$, being expanded in a Fourier series

$$\rho(r) = \sum_g \rho_g \, e^{ig \cdot r} \tag{2.1}$$

where the vectors g are reciprocal lattice vectors of the periodically replicated simulation system. Velocities and non-physical 'masses' μ_g are allocated to the Fourier coefficients. Coupled equations of motion are then derived for both the ion positions $\{R_\alpha\}$ and the electronic coefficients ρ_g:

$$\mu_g \ddot{\rho}_g = -\frac{\delta E}{\delta \rho_g} \qquad |g|^2 \leqslant 2E_c \tag{2.2}$$

and

$$M_I \ddot{R}_\alpha = -\nabla_\alpha E - \nabla_\alpha V_{II} \qquad \alpha = 1, \ldots, N_I \tag{2.3}$$

where V_{II} is the potential energy of the direct ion–ion interaction and the electronic energy E is a functional of $\rho(r)$ for a given $\{R_\alpha\}$. N_I is the number of ions, and E_c the energy cut-off for the plane wave expansion. Molecular dynamics simulations are performed by simultaneously integrating these equations of motion with the ρ_g appropriate to the electronic ground state.

As in the majority of Car–Parrinello-style simulations, $E[\rho]$ is provided by density functional theory [13]. However, for the reasons given above, the kinetic energy functional is constructed without the introduction of orbitals. How this is done, following the work of Perrot [14] and similar developments by Wang and Teter [15], is described in detail in [11]. The remainder of the energy functional comprises the interaction of the electron density with the ion potential (represented by the Topp–Hopfield pseudopotential [16]), the coulombic electron–electron interaction and the local exchange–correlation functional of Ceperley and Alder [17].

A simulation was performed on a system of 128 sodium atoms at 388±18 K with number density 0.0241 $Å^{-1}$ (as used in [18]), in a cubic cell with periodic boundary conditions, and starting from a previously equilibrated liquid configuration. The run was for 96 ps, taking around 250 h of CPU time on a Convex C2 [19]. The molecular dynamics timestep was 4.8×10^{-4} ps, half that used in simulating the solid [10]. The plane-wave cut-off was 11.7 Ryd, larger than that used in the solid state work. These conservative choices of parameters were found to be necessary to avoid energy drift over the extremely long run length. A shortcoming of simulations using the Car–Parrinello algorithm in the Kohn–Sham

scheme is that energy can leak from the electronic to the ionic degrees of freedom in metallic systems, for reasons discussed in [5]. This can be cured by the introduction of 'thermostats' which control the 'temperatures' of the two subsystems [20, 21], at a cost of, at least, some elegance. Reference [10] describes how the present technique is able to minimize this 'non-adiabaticity' problem by adjusting the fake masses assigned to the electronic degrees of freedom so as to widely separate the frequencies of coefficient and ionic motions ('conditioning' the algorithm). The target value for the coefficient frequencies was around 580 ps^{-1}. The combination of conservative step length, more accurate representation of the electrons and conditioning meant that no thermostatting was required: we did requench the electronic degrees of freedom three times during the course of the run, but this had no discernible effect on the ionic trajectories.

3. Calculation of observable properties

The properties of the simulated fluid were studied by means of various correlation functions, some of which are also obtainable from neutron and x-ray scattering experiments. The calculated quantities were Fourier coefficients of certain densities and were obtained for a range of wavevectors ($\boldsymbol{k}$) consistent with the periodic boundary conditions. The correlation functions were averaged over vectors of equal magnitude k (as the liquid is isotropic).

3.1. Static structure factor and x-ray diffraction

The static structure factor

$$S(k) = \frac{1}{N_I}\left\langle \left(\sum_{\alpha=1}^{N_I} e^{-i\boldsymbol{k}\cdot\boldsymbol{R}_\alpha(t_0)}\right)\left(\sum_{\alpha=1}^{N_I} e^{i\boldsymbol{k}\cdot\boldsymbol{R}_\alpha(t_0)}\right)\right\rangle \tag{3.1}$$

is shown in figure 1 in comparison with data from an x-ray scattering experiment conducted on liquid sodium at 373 K [22]. The simulation values are calculated directly as indicated in the equation, rather than by transformation of the radial distribution function, so as to avoid truncation errors. It can be seen that the overall agreement is excellent, except for the height of the first peak, which is overestimated. The figure shows results for $S(k)$ averaged over a relatively short interval at the start of the run, over the first half of the run and over the full run. It can be seen that the peak has been growing and/or shifting to slightly lower k as the run progresses. One k point at the second peak becomes slightly more pronounced as well but the remaining points are unchanged. The increasing sharpness of the first peak implies that the simulated fluid is developing longer-range order at this wavevector than is present in the real fluid. We believe that we are seeing an artifact of the small system size, exacerbated by the proximity of the simulated fluid to its solid phase. Given that 128 atoms can form a body-centred cubic lattice in a cubic box, that the density of sodium changes by only around 2% on freezing, and that we are in the vicinity of the freezing point of sodium, we may be observing incipient solid-like order induced by the periodic boundary conditions. The k vector which is affected by this is the one at the position where the first Bragg peak would appear for a lattice of solid sodium at our system's density. However, the Bragg peak for a perfect crystal would have a height of 128, so the extent of the enhancement we see (of about 0.5) suggests that any such effect is only small. We do not believe that this artefact is a consequence of the *ab initio* nature of the simulation. Indeed simulation studies of liquid metals close to freezing which use effective interionic interactions have often shown an enhancement of $S(k)$ at its first maximum over experiment

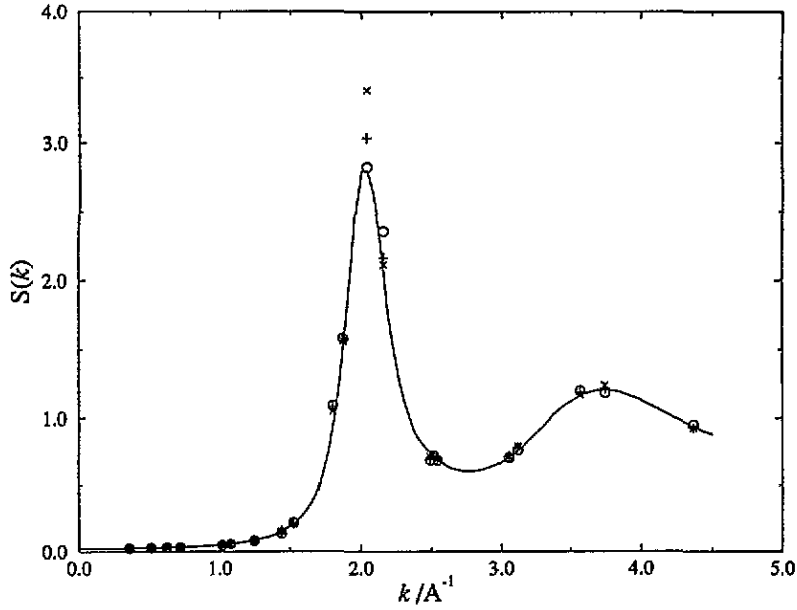

Figure 1. The experimental static structure factor, from x-ray measurements [22], is compared with the simulation results. The symbols denote values calculated by averaging over different portions of the run: ○, first 25 ps; +, first 50 ps; ×, full run (96 ps).

[23]. *If our reasoning is correct, the simplest way to avoid the artefact would be to use a* particle number which could not crystallize in the simulation cell and to use more particles.

3.2. Dynamic structure factors and neutron scattering

Foremost amongst the correlation functions used to examine the dynamic properties of the system is the intermediate scattering function

$$F(k,t) = \frac{1}{N_I}\left\langle \left(\sum_{\alpha=1}^{N_I} e^{-ik\cdot R_\alpha(t+t_0)}\right)\left(\sum_{\alpha=1}^{N_I} e^{ik\cdot R_\alpha(t_0)}\right)\right\rangle \tag{3.2}$$

which on Fourier transformation yields the dynamic structure factor $S(k,\omega)$.

The time transform was taken over a correlation length of 1.50 ps. Multiplication with a Blackman windowing function [24] was performed so as to remove effects due to the finite length of the correlation function and then Fourier transformation was carried out numerically by the Filon method [24]. Although the functions were calculated out to much longer times, in the hope of obtaining high resolution in frequency space, we observed that they became quite noisy at times longer than about 1.5 ps, despite the long run length. We attribute this to the propagation of disturbances between periodic images. Using such a short correlation length means that the frequency resolution in the dynamic structure factor is only of order 1–2 ps^{-1}. The resulting dynamic structure factor is displayed in figure 2: it is clear that any significant structure in this function occurs at frequencies higher than 2–3 ps^{-1} and is thus unaffected by the windowing process.

There is a clear Brillouin peak at around 10 ps^{-1} for the smallest k vector. This persists almost up to the principal peak of the structure factor, showing the presence of collective motions in the fluid at these wavevectors, but it is not observed beyond the principal peak.

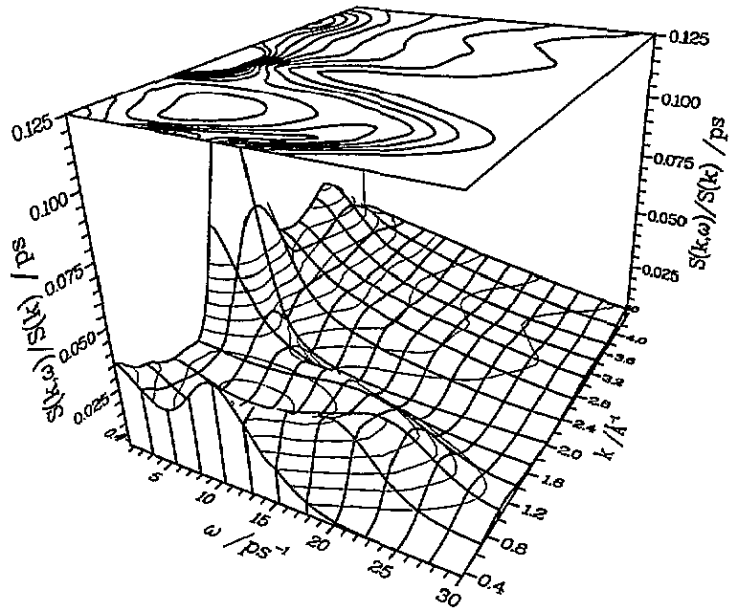

Figure 2. The simulated dynamic structure factor, $S(k, \omega)$, in a 3D representation and with a superimposed contour plot.

The persistence of a Brillouin peak up to much higher wavevectors than observed in ionic or atomic fluids is a well known property of metallic liquids [25].

In principle [26], $S(k, \omega)$ is experimentally obtainable from coherent neutron scattering. In practice, the neutron scattering experiments on sodium have not been able to separate the coherent from the incoherent scattering as cross-sections for sodium, σ_c and σ_i, are of the same order ($\sigma_c = 1.66$ barns, $\sigma_i = 1.74$ barns) [27]. What is immediately accessible is the *effective* dynamic structure factor

$$S_e(k, \omega) = \frac{\sigma_c S(k, \omega) + \sigma_i S_s(k, \omega)}{\sigma_c + \sigma_i} \tag{3.3}$$

where $S_s(k, \omega)$ is the the self-dynamic structure factor arising from the incoherent scattering and is the Fourier transform of the self-intermediate scattering function:

$$F_s(k, t) = \frac{1}{N_1} \sum_{\alpha=1}^{N_1} \langle e^{-i\mathbf{k}\cdot\mathbf{R}_\alpha(t+t_0)} e^{i\mathbf{k}\cdot\mathbf{R}_\alpha(t_0)} \rangle. \tag{3.4}$$

Such data have been presented in [18].

We have constructed the effective dynamic structure factor from our simulation data using equation (3.3), where $S_s(k, \omega)$ was obtained by numerical Fourier transform of the 12 ps long self-correlation function after multiplication with a Blackman window. (No problems with interference from periodic images are encountered in the self-correlation.) The comparison with experiment over the range of k probed experimentally is shown in figure 3. In practice, because of the fact that the amplitude of $S(k)$ is low except at the largest k value, and because $S(k, \omega)$ is much broader that $S_s(k, \omega)$, the shape of these functions is dominated by the incoherent scattering.

Agreement with experiment is very good for most of the range, except at the largest value of k. Even at this k value, if the amplitude of the simulated function is suitably

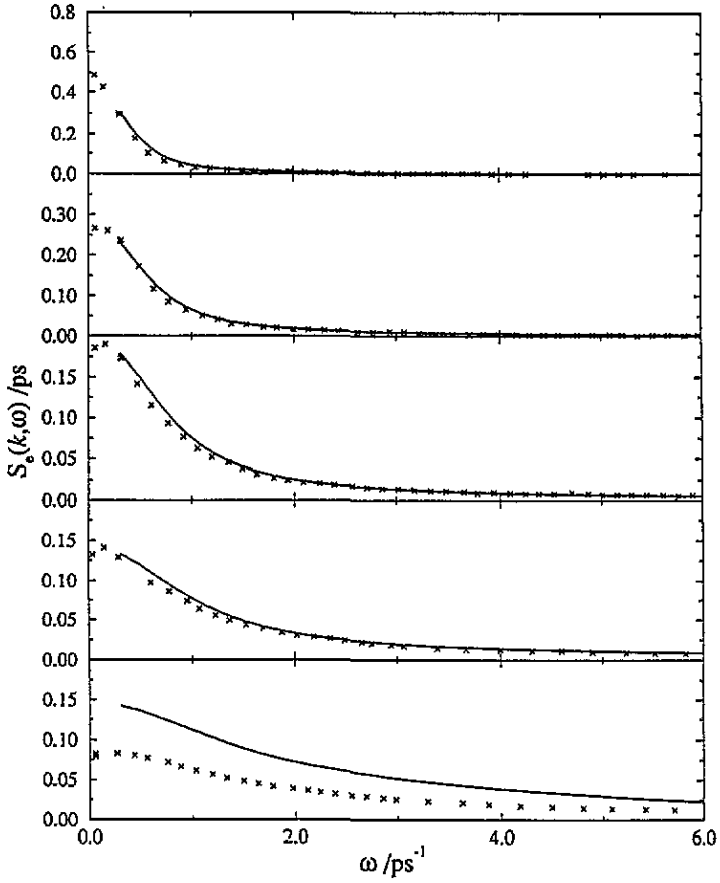

Figure 3. The effective dynamic structure factor, $S_e(k, \omega)$, obtained from neutron scattering (crosses, [17]) is compared with the simulation results (full lines) at several k values. From top to bottom the (experimental, simulation) k values (Å^{-1}) are (0.69, 0.72), (0.94, 1.02), (1.25, 1.25), (1.53, 1.53), and (1.80, 1.80).

scaled, the experimental and simulated curves are brought into excellent agreement; the disagreement apparent in the bottom panel of figure 3 is therefore one of amplitude. The relevant k value lies on a part of $S(k, \omega)$ which is very steep with respect to k because of the proximity to the principal peak of $S(k)$, and so the coherent contribution to $S_e(k, \omega)$ would be expected to be very sensitive to small discrepancies in $S(k)$. However, to give the error in amplitude apparent in the bottom panel of figure 3 the error in $S(k)$ at this value of k would have to be of order 100%, rather than the ~5% apparent from figure 1, and changing the amplitude of the coherent relative to the incoherent scattering would change the spectral shape for which the agreement is good. It seems to us that the experimental amplitude is unreasonably low. At $k = 1.53$, for which $S_e(k, \omega)$ is shown in the next higher panel of figure 3, the effective scattering is dominated by $S_s(k, \omega)$. At $\omega = 0$ the amplitude of $S_s(k, \omega)$ should vary as k^{-2}. The experimental value of $S_e(k, 0)$ at $k = 1.80$ is *lower* than would be expected from the scaling $k = 1.53$ data, i.e. lower than the expected incoherent scattering *alone*, without allowing for the coherent contribution.

Even though $S_s(k, \omega)$ has not been separately resolved from experiment, attempts have been made to recover it indirectly at very low energy transfer through the use of an estimate of the coherent contribution to the measured effective dynamic structure factor [28, 29].

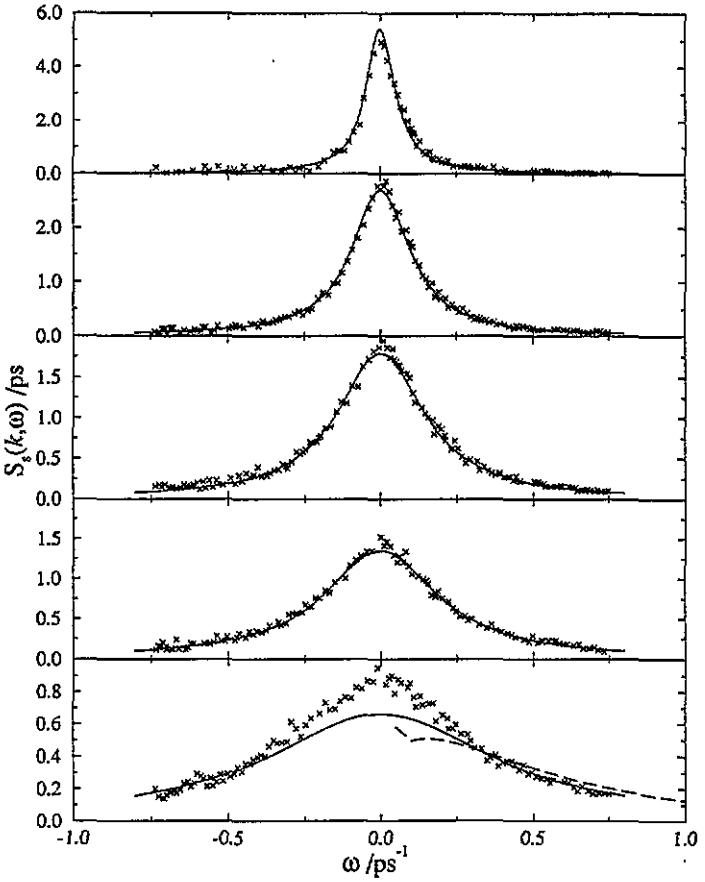

Figure 4. Comparison of experimental self-dynamic structure factors [28, 29], shown as crosses, with simulation values at several values of k. From top to bottom the (experimental, simulation) k values (Å^{-1}) are (0.383, 0.360), (0.518, 0.509), (0.648, 0.624), (0.740, 0.720), and (0.966, 1.02). The bottom panel also shows the simulation data transformed by truncation and Blackman windowing at 12 ps (dashed line).

Such data from a very recent neutron scattering experiment [29] are presented in figure 4 and compared with simulation data. Since the neutron data are reported at very low frequency the simulated $S_s(k, \omega)$ was obtained by fitting the calculated $F_s(k, t)$ to an exponential function for times in the range 3–8 ps and using this exponential to extend the range of integration in calculating the transform. Over the range 1–12 ps this fit was excellent and could not be systematically improved by choice of any other function. The transform was calculated by combining the analytic transform of the exponential with the numerical transform of the residue of the fit. Doing the transform in this way allowed comparison to be made with the very small values of ω where experimental data is available. In the bottom panel of figure 4, the value of $S_s(k, \omega)$ obtained from a direct transform of $F_s(k, t)$ Blackman windowed over the 12 ps range is shown, to illustrate the ω value at which the extrapolation procedure becomes significant.

Good agreement is found between simulation and experiment on the shape, width, and amplitude of $S_s(k, \omega)$ showing that the diffusive behaviour indicated by the exponential representation of the simulation data is realistic. The greatest discrepancy is found at $k \simeq 1$ Å (bottom panel of figure 4), although this can be partially attributed to the difference in k

vector used in simulation and experiment. Notice that our agreement with the experimental data, for $S_e(k, \omega)$, is good around this value of k.

3.3. Current correlation functions

Also calculated from the simulation were the longitudinal and transverse current correlation functions

$$C^{l}(q,t) = \left\langle \left(\sum_{\alpha=1}^{N_I} \frac{\boldsymbol{k}\cdot\boldsymbol{v}_I(t+t_0)}{q} e^{-i\boldsymbol{k}\cdot\boldsymbol{R}_\alpha(t+t_0)} \right) \left(\sum_{\alpha=1}^{N_I} \frac{\boldsymbol{k}\cdot\boldsymbol{v}_I(t_0)}{q} e^{i\boldsymbol{q}\cdot\boldsymbol{R}_\alpha(t_0)} \right) \right\rangle \tag{3.5}$$

and

$$C^{t}(q,t) = \left\langle \left(\sum_{\alpha=1}^{N_I} \left(\boldsymbol{v}_I(t+t_0) - \frac{\boldsymbol{k}\cdot\boldsymbol{v}_I(t+t_0)}{q\cdot q}\boldsymbol{k} \right) e^{-i\boldsymbol{k}\cdot\boldsymbol{R}_\alpha(t+t_0)} \right) \times \left(\sum_{\alpha=1}^{N_I} \left(\boldsymbol{v}_I(t_0) - \frac{\boldsymbol{k}\cdot\boldsymbol{v}_I(t_0)}{q\cdot k}\boldsymbol{k} \right) e^{i\boldsymbol{k}\cdot\boldsymbol{R}_\alpha(t_0)} \right) \right\rangle \tag{3.6}$$

The Fourier transformation was performed as for $S(k, \omega)$. The positions of the maxima of the peaks ω_l^{max} and ω_t^{max} in the Fourier transforms of these functions provide curves analogous to phonon dispersion curves for the solid [26]. These are shown in figures 5 and 6. These curves have the same form as seen in other simulations of alkali metals [30] and, for ω_l^{max}, with values which have been deduced from the peaks seen in $\omega^2 \times S(k, \omega)$ from experimental scattering data [31]. These peaks have been attributed to the persistence of propagating sound modes even at these very high values of k, as anticipated from certain theories [33].

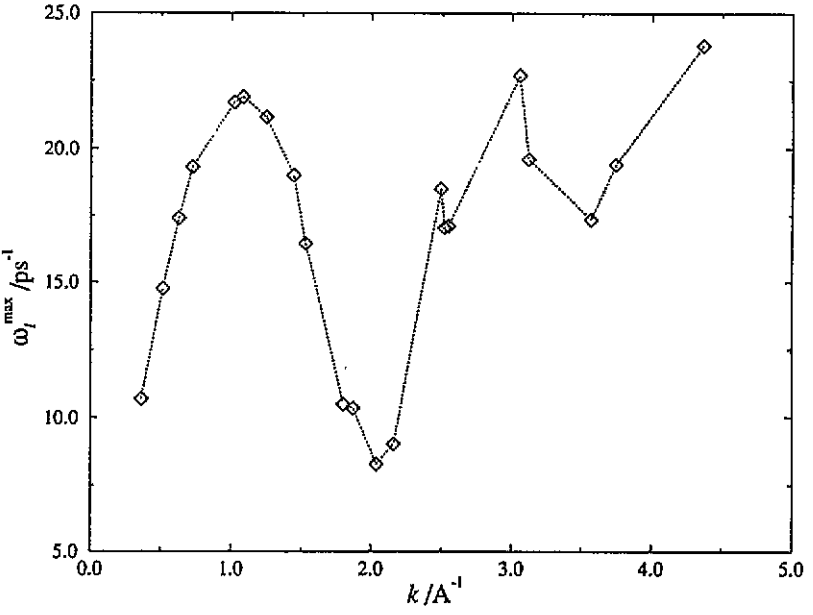

Figure 5. The position of the peak in the spectrum of the longitudinal current correlation function. Note the close similarity to the behaviour of the contours in figure 2.

One feature of interest, which might be seen in our data, is a 'Kohn anomaly' [32] in the 'dispersion curves' due to the singularity in the electronic reponse function caused by

Fermi surface effects. This occurs at a wavevector equal to twice the Fermi wavevector, or $2k_F = 1.79$ Å^{-1} at the density we have studied. Because of the *ab initio* nature of our simulation, the origins of the anomaly are properly represented. Examination of figure 5 shows that any Kohn anomaly in the Brillouin peak position would be very difficult to observe, since $2k_F$ is very close to the position of the first peak in the dynamic structure factor and hence the Brillouin peak is at very low frequency and very strongly damped. Our data are suggestive of a kink in ω_l^{max} at $2k_F$, but it should be remembered that ω_l^{max} has been extracted from the data as the position of a peak in a fairly broad spectral function. Figure 6 shows that ω_t^{max} does exhibit a sharp peak at $2k_F$: unfortunately, this function is not experimentally observable in a fluid. It would be interesting to compare this behaviour with that found in a sodium simulation with an effective pair potential, which should not show a Kohn anomaly.

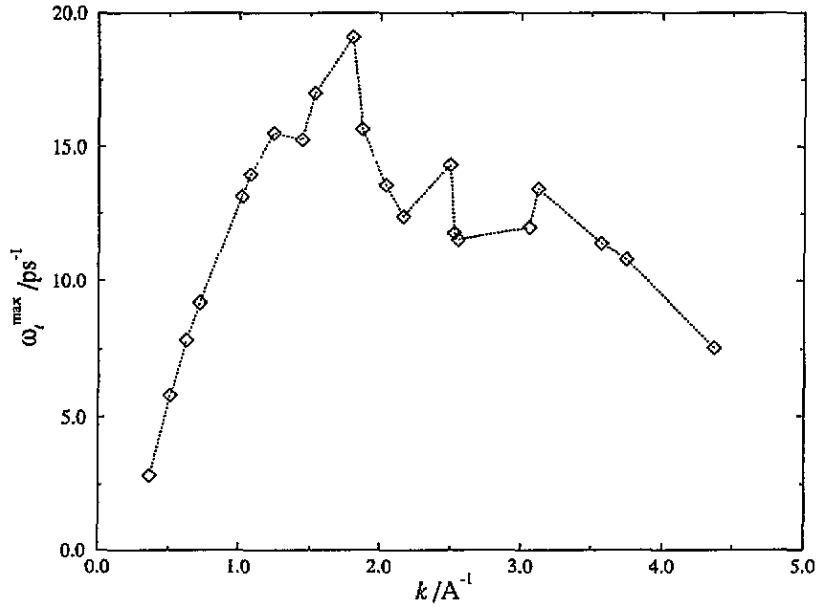

Figure 6. The position of the peak in the spectrum of the transverse current correlation function.

4. Discussion

The primary purpose of this paper has been to show that *ab initio* methods can be used to simulate the dynamical properties of liquids in the same manner as in conventional simulations based on effective internuclear potentials and at the level of statistical precision achieved in experiments. This is the first time *ab initio* techniques have been used to obtain comprehensive dynamical information about this—or indeed, any—liquid system. For the most part, agreement with experiment is excellent. We have carefully discussed all apparent discrepancies between the simulated and experimentally observed behaviour: only in the case of the anomalously high peak in $S(k)$ do we believe the discrepancy to be due to simulation methodology and here we anticipate that by working with a different number of particles we would eliminate even that.

Ideally, the only input to a calculation of the type we have described is the atomic number of sodium. However, we have fallen short of that ideal in two regards. We made use of the Topp–Hopfield pseudopotential because of its desirable computational properties and because it gives a good account of the properties of the solid; however, this is not a true *ab initio* potential. Secondly, we performed the calculations at the experimental liquid density at the melting point. In practice our simulated system is under a pressure of about 3 kbar at this density. The source of this error could be associated with the pseudopotential, and further work is in progress with *ab initio* potentials to examine this possibility. However, the error corresponds to an overestimate of the lattice parameter of the solid of about 2%, which is typical of calculations which use the local density approximation to to the exchange and correlation functionals and it may be that this represents the real limitation on accuracy.

In order to accomplish the calculations in a reasonable amount of time, we have made use of a kinetic energy functional which has a restricted range of applicability (but does give an excellent representation of solid sodium). The calculations otherwise employ exactly the methods laid down by Car and Parrinello in their classic paper. Similar dynamical calculations will become possible for more 'interesting' fluids than sodium both by further developments in the orbital-free functional scheme, which will expand its domain of applicability without sacrificing the advantages which we have sought to illustrate, and by improvements in Kohn–Sham methodology and computer technology.

The reason for regarding liquid sodium close to its freezing point as not 'interesting' is that it has already been successfully treated using conventional simulation methods [18, 34, 23] with effective pair potentials derived from empirical pseudopotentials [35]. The relationship of our methodology to that used in deriving effective potentials for metals was discussed in [11]. The quality of agreement with experiment reached in the best of these calculations is quite comparable to that we have demonstrated here.

Acknowledgments

We thank Professor C Morkel for sending us the incoherent neutron scattering data before publication. The work was supported by SERC and the MOD (UK) under grant GR/H38256. It has also benefitted from further support from SERC under grant No GR/H10276. Michael Foley is grateful to the Association of Commonwealth Universities for the award of a Commonwealth Scholarship.

References

[1] Car R and Parrinello M 1985 *Phys. Rev. Lett.* **55** 2471
[2] Galli G and Pasquarello A 1993 *Computer Simulation in Chemical Physics* ed M P Allen and D J Tildesley (Dordrecht: Kluwer)
[3] Kohn W and Sham L J 1965 *Phys. Rev.* **140** A1133
[4] Remler D K and Madden P A 1990 *Mol. Phys.* **70** 921
[5] Pastore G, Smargiassi E and Buda F 1991 *Phys. Rev.* A **44** 6334
[6] Payne M C, Teter M P, Allen D C, Arias T A and Joannopoulos J D 1992 *Rev. Mod. Phys.* **64** 1045
[7] Galli G and Parrinello M 1992 *Phys. Rev. Lett.* **69** 3547
[8] Baroni S and Gianozzi P 1992 *Europhys. Lett.* **17** 547
[9] Li X P, Nuñes W and Vanderbilt D 1993 *Phys. Rev.* B **47** 10891
[10] Pearson M, Smargiassi E and Madden P A 1993 *J. Phys.: Condens. Matter* **5** 3221
[11] Smargiassi E and Madden P A 1994 *Phys. Rev.* B **49** 5220
[12] Smargiassi E and Madden P A *Phys. Rev.* B submitted

[13] Parr R G and Yang W 1989 *Density-Functional Theory of Atoms and Molecules* (Oxford: Oxford University Press)
[14] Perrot F 1994 Private communication
[15] Wang L W and Teter M P 1992 *Phys. Rev.* B **45** 13 197
[16] Topp W C and Hopfield J J 1973 *Phys. Rev.* B **7** 1295
[17] Ceperley D M and Alder B J 1980 *Phys. Rev. Lett.* **45** 566
Perdew J P and Zunger A 1981 *Phys. Rev.* B **23** 5048
[18] Kinell T, Dahlborg U, Söderström O and Ebbsjö I 1985 *J. Phys. F: Met. Phys.* **15** 1033
[19] Further improvements to the code since this run was made would make the run time 90 h on an IBM RS6000 model 320H, using the ESSL library for the Fourier transforms.
[20] Fois E S, Penman J N and Madden P A 1993 *J. Chem. Phys.* **98** 6361
[21] Blöchl P E and Parrinello M 1992 *Phys. Rev.* B **45** 9413
[22] Greenfield A J, Wellendorf J and Wiser N 1971 *Phys. Rev.* A **4** 1607
[23] Shimojo F, Hoshino K and Watabe M 1994 *J. Phys. Japan* **63** 141
[24] Allen M P and Tildesley D J 1987 *Computer Simulation of Liquids* (Oxford: Clarendon)
[25] Jacucci G and McDonald I R 1980 *Liquid and Amorphous Metals* ed E Lüscher and H Coufal (Amsterdam: Sijthoff and Noordhoff)
[26] Hansen J P and McDonald I R 1986 *Theory of Simple Liquids* (London: Academic)
[27] Söderström O and Dahlborg U 1984 *J. Phys. F: Met. Phys.* **14** 2297
[28] Morkel C and Gläser W 1986 *Phys. Rev.* A **33** 3383
[29] Stangl A 1993 *Ph D Thesis* Technishche Universität München
[30] Kambayashi S and Kahl G 1992 *Phys. Rev.* A **46** 3255
[31] Winter R, Pilgrim C, Morkel C and Glaser W 1993 *J. Non-Cryst. Solids* **156–158** 9
[32] Ashcroft N W and Mermin N D 1976 *Solid State Physics* (Philadelphia, PA: Holt–Saunders)
Harrison W A 1970 *Solid State Theory* (New York: McGraw-Hill)
[33] de Schepper I M and Cohen E G D 1982 *J. Stat. Phys.* **27** 123
[34] Balucani U, Torcini A and Vallauri R 1993 *Phys. Rev.* B **47** 3011
[35] Hafner J 1987 *From Hamiltonian to Phase Diagrams* (Berlin: Springer)